Physica D 58 (1992) 31–49
North-Holland

PHYSICA D

Distinguishing between low-dimensional dynamics and randomness in measured time series

A. Provenzale[a], L.A. Smith[b], R. Vio[c] and G. Murante[a]

[a]*Istituto di Cosmogeofisica del CNR, Corso Fiume 4, I-10133 Turin, Italy*
[b]*Department of Engineering, Warwick University, Coventry CV4 7AL, UK*
[c]*Dipartimento di Astronomia, Università di Padova, V.lo Dell'Osservatorio 5, I-35122 Padua, Italy*

Received 5 November 1991
Revised manuscript received 2 March 1992
Accepted 2 March 1992

The success of current attempts to distinguish between low-dimensional chaos and random behavior in a time series of observations is considered. First we discuss stationary stochastic processes which produce finite numerical estimates of the correlation dimension and K_2 entropy under naive application of correlation integral methods. We then consider several straightforward tests to evaluate whether correlation integral methods reflect the global geometry or the local fractal structure of the trajectory. This determines whether the methods are applicable to a given series; if they are we evaluate the significance of a particular result, for example, by considering the results of the analysis of stochastic signals with statistical properties similar to those of observed series. From the examples considered, it is clear that the correlation integral should not be used in isolation, but as one of a collection of tools to distinguish chaos from stochasticity.

1. Introduction

In the past ten years, a variety of methods to extract phase space dynamical information from experimentally observed or computer generated time series have been developed, see e.g. refs. [1–28]. These methods are generally based on a phase space reconstruction (typically a "time embedding" procedure, see refs. [22, 29]) and are devoted to the calculation of the properties of a (supposed) underlying attractor (such as the correlation dimension [12, 14, 20, 23, 25], the K_2 entropy [13] and the Lyapunov exponents [1, 9, 18, 28]), to the determination of the approximate number of the (empirical) modes excited in the system through singular value decomposition (SVD) [3], to the issue of predicting the future evolution of the system from the knowledge of its past, in a spirit which is the extension of classical autoregressive (AR) approaches [5, 10, 11, 21, 30], or even toward reconstructing the equations of motion of the system [7, 10].

The "static" methods based on the correlation integral [12–14, 24, 25] differ from prediction methods in that the former do not explicitly take into account information from the ordering of the points in the time series. The methods mentioned above provide information on systems which are known to be dominated by low-dimensional deterministic dynamics and there exists a noticeable difference in the results from low-dimensional chaotic systems and uncorrelated (white) noise. Applications to well-controlled laboratory experiments have led to determining the presence of low-dimensional chaos in several experimental contexts, see e.g. refs. [31–33]; note that these systems were characterized by a limited degree of space complexity and by the ability to adjust control parameters.

The situation turns out to be much more com-

plicated for natural (uncontrolled) systems, see e.g. refs. [34–46], where claims and counterclaims for low-dimensional attractors coexist for the same data, as well as for systems dominated by the presence of "colored" noises with power-law power spectra [43, 47–49] or for non-linear stochastic processes [27]. In this paper we briefly review some of the problems encountered in the study of systems characterized by the presence of correlated stochastic processes and we discuss a few simple tests which can be of use in the attempt of distinguishing between low-dimensional (dissipative) determinism and stochastic noise.

2. Behavior of correlated noises

The majority of quantitative attempts to detect low-dimensional attractors from time series data have focused on the estimation of the correlation dimension and of the correlation entropy K_2. Given a scalar time series $x(t_i)$, the first step in the analysis is to employ an embedding procedure to reconstruct the system phase space. Here we consider the method of delays [22, 29], where a vector time series is defined as

$$\boldsymbol{x}(t_i) = \{x(t_i), x(t_i + \tau), \ldots, x(t_i + (M-1)\tau)\} . \tag{2.1}$$

Here $\tau = m\,\Delta t$ is an appropriate time delay, Δt is the effective sampling time and M is the dimension of the vector $\boldsymbol{x}(t_i)$. Recent discussions of embedology are given in refs. [6, 19]. The crucial idea underlying the embedding procedure (2.1) is that the observed variable $x(t)$ contains information on all the other phase space variables of the system. In the case of weakly coupled phase space variables, however, the above method may lead to misleading results [40]. Note that the choice of the time delay τ is somewhat arbitrary [17, 50]; there may not even be a unique good selection criterion for this parameter [15].

The correlation integral $C_M(r)$ of the reconstruction is defined as [12]

$$C_M(r) = \frac{1}{N'^2} \sum_{i;j}^{N'} \theta\{r - \|\boldsymbol{x}(t_i) - \boldsymbol{x}(t_j)\|\} , \tag{2.2}$$

where θ is the Heaviside step function, N is the number of points in the time series, $N' = N - m(M-1)$ and the vertical bars indicate the norm of the vector. Efficient implementations of (2.2) are available [14, 24] and a clear overview of the analysis is presented in ref. [25]. One is then interested in the scaling properties of the correlation integral, in particular whether $C_M(r)$ is a power-law at small scales, that is

$$C_M(r) \underset{N\to\infty, r\to 0}{\sim} r^{\nu_M} , \tag{2.3}$$

where we have ignored any effects due to lacunarity [2, 51]. If (2.3) holds, the next step is to examine the behavior of the estimated correlation exponent ν_M with increasing M. For point distributions with a low-dimensional geometry, one may show that at sufficiently large M [6, 8, 12]

$$\nu_M \to \nu , \tag{2.4}$$

where ν is the correlation dimension; for *deterministic* dynamical systems, this quantity provides an estimate of the number of degrees of freedom excited in the system. We stress that eqs. (2.3) and (2.4) assume a very large data set and that the results should be independent of τ over an appropriate range of values.

The K_2 entropy [13] may be estimated from the correlation integrals $C_M(r)$. This is computed (in the limit as $M \to \infty$) as the distance between two successive correlation integrals in log–log coordinates. Specifically

$$\frac{1}{\Delta t} \log \frac{C_M(r)}{C_{M+1}(r)} \underset{r\to 0}{\sim} K_2(M) \tag{2.5}$$

and then

$$K_2(M) \underset{M\to\infty}{\sim} K_2 . \tag{2.6}$$

The K_2 entropy is zero for periodic or quasi-periodic systems, it is positive for chaotic systems and diverges for a white noise. Since low-dimensional strange attractors *do* produce a small and usually non-integer value of the correlation dimension and a converging K_2 entropy, the above statements have on occasion been reversed and a finite, small value of the correlation dimension and a converging K_2 entropy have been taken as "proof" of the presence of a strange attractor. As a counterexample to this belief, Osborne and Provenzale [47], and Provenzale et al. [48] have shown that simple stochastic processes, characterized by a power-law power spectrum with random, independent, uniformly distributed Fourier phases, generate time series with finite correlation dimension and converging K_2 entropy estimates, both of which are determined by the logarithmic spectral slope.

The stochastic signals considered in refs. [47, 48] are defined through their Fourier representation, i.e., by

$$x(t_i) = \sum_{k=1}^{N/2} A(\omega_k) \cos(\omega_k t_i + \phi_k) , \quad i = 1, N ,$$
$$A^2(\omega_k) \propto \omega_k^{-\alpha} , \tag{2.7}$$

where $\omega_k = 2\pi k / N \Delta t$ and the ϕ_k are random uncorrelated phases. The "saturation" value of the correlation dimension ν is determined by the logarithmic spectral slope α through $\nu = 2/(\alpha - 1)$ for $1 < \alpha < 3$ [47]. In addition, the numerical estimates of the K_2 entropy were found to be convergent when $\alpha > 1$ [48]. The extension of these results to systems whose power spectrum has a power-law behavior only on a limited frequency range has been considered by Theiler [49]. A similar problem was also considered by Harding et al. [37], who studied a stochastic signal generated by a random walk in Fourier space which leads to a finite value of the correlation dimension. Clearly, the noises (2.7) are not associated with any low-dimensional system. The above results simply show that the standard time-embedding techniques and dimension and entropy calculations should not be used without a careful evaluation of the conditions for their applicability and an examination of the consistency of the results obtained. A naive application of these methods may lead to erroneous conclusions.

The colored noise example discussed above is certainly not the only class of random noises which give a finite estimate of ν and a convergent K_2 when finite-time series are considered [27, 49]. Following Vio et al. [27], we consider the two time series generated by a *linear* and by a *non-linear* stochastic process, given respectively by

$$\frac{dx}{dt} = \theta x(t) + w(t) , \tag{2.8}$$

$$\frac{dy(t)}{dt} = (\alpha - 0.5)\beta - y(t) + [2\beta y(t)]^{1/2} w(t) , \tag{2.9}$$

where $w(t)$ is a standard gaussian white noise process. Two such time series are shown in figs. 1a (linear case) and 1b (non-linear case) for the parameter values $\theta = -0.9$ and $\alpha = \beta = 1$. The discrete version of the process in formula (2.8) is a classical AR(1) linear model; the numerical integration of eq. (2.9) is pursued by the local linearization method of Ozaki [52] with $\Delta t = 0.02$ for both series. Unless noted otherwise, we consider time series composed of $N = 4000$ data points. This corresponds to a length of about 15 correlation times, similar to signals commonly encountered in the study of natural systems.

Both the linear and the non-linear processes (2.8) and (2.9) generate *stationary* time series for parameters values in an appropriate range [27]. It is important to note that both the linear and the non-linear time series possess very similar power spectra (a power-law power spectrum $P(\omega) \approx \omega^{-2}$ over a large frequency range) and very similar structure functions (defined below). As shown in ref. [27], the two series differ in that the linear signal $x(t)$ is statistically self-similar

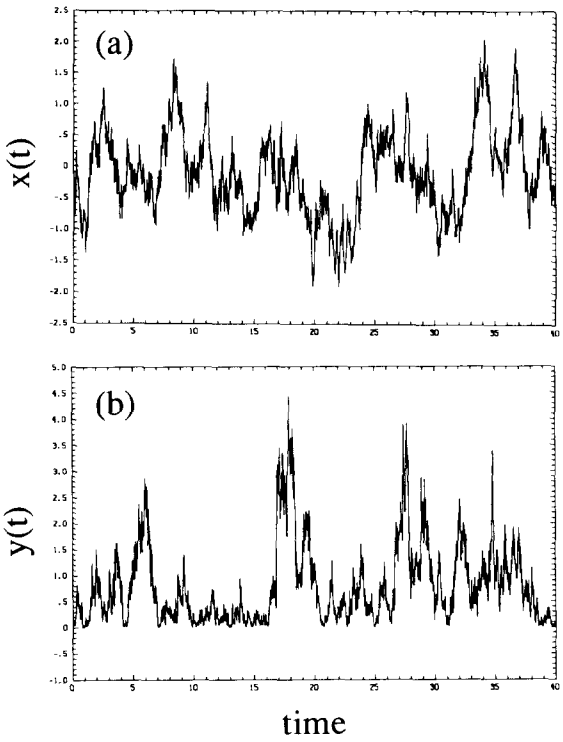

Fig. 1. (a) Time series obtained from the linear stochastic process (2.8) with $\theta = -0.9$ and $\Delta t = 0.02$. (b) Time series generated by the non-linear stochastic process (2.9) with $\alpha = \beta = 1$ and $\Delta t = 0.02$.

(an homogeneous fractal signal), while the non-linear signal $y(t)$ is multifractal and intermittent. This is reflected by the fact that the Fourier phases of the linear system (2.8) are random uniformly distributed with no correlation with each other, while some of the Fourier phases of the non-linear signal (2.9) have a non-zero correlation, as revealed for example by the bispectrum analysis. This implies that the stochastic signal given by formula (2.8) has close analogies with those studied in refs. [47, 48], while the signal (2.9) is a truly new entity.

Figs. 2a and 2b report the correlation integrals for the linear and non-linear time series respectively; figs. 2c and 2d show the correlation exponent ν_M and $K_2(M)$ versus the embedding dimension for the two time series, as computed by linear least-squares fit of $\log C_M(r)$ versus $\log r$ on the scaling range $0.002 \leq C_M(r) \leq 0.02$. Note the "knee" in the correlation integrals for large M, at a value $C_M(r) \approx 0.02$, consistent with the results by Theiler [49] on stationary random processes with a power-law spectrum on a finite frequency range. The procedure of phase space reconstruction and the subsequent dimension and entropy calculations give the similar value $\nu \approx 2.5$ (at embedding dimension $M = 8$) and an equally converging K_2 entropy for both time series, independent on the linear or non-linear nature of the signals. For both signals, the time delay τ used in the time embedding procedure, $\tau = 250\,\Delta t$, is near the first zero of the autocorrelation function. In any event, the convergence of the correlation dimension and of the entropy does not significantly depend on the choice of the time delay over a large range of values of τ.

The computed value of the correlation dimension for both signals is slightly larger than the value indicated by the expression $\nu = 2/(\alpha - 1) = 2$ when $\alpha = 2$. This is due to the fact that the power spectrum of the signals (2.8) and (2.9) tend to become flat at low frequencies, consistent with the stationary nature of the processes [27]. When the length of the time series increases, the noises (2.8) and (2.9) tend to become space-filling, as required for stationary stochastic processes. However, this convergence is slow, and for a finite number of points an apparently finite estimate of the correlation dimension is typically obtained. Increasing the length of the signal produces somewhat larger estimates of the dimension. Clearly, an increase of the dimension estimates with the length of the time series should warn about misleading conclusions; unfortunately, such a test is often not available in the study of natural systems.

In the case of noises with a power-law spectrum and a low-frequency cutoff ω_0 (below which the spectrum becomes flat), Theiler [49] has recently derived an analytic expression for the correlation integral; the existence of different scaling regimes at different scales has been detected, the fractal behavior being associated with

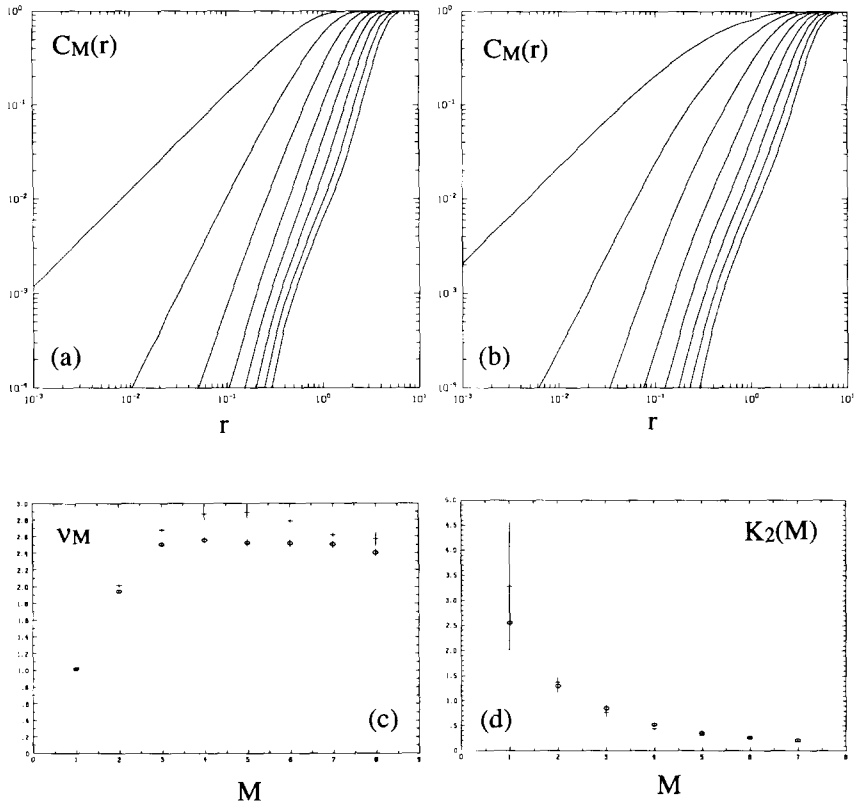

Fig. 2. (a) and (b) report the correlation integrals $C_M(r)$ for the linear (2.8) and non-linear (2.9) stochastic processes shown in fig. 1. The time delay τ in the embedding procedure has been chosen to be $\tau = 250\,\Delta t$, approximately corresponding to the first zero of the autocorrelation of the signals. The embedding dimension varies from $M = 1$ to $M = 8$. (c) and (d) report the correlation exponent ν_M and the correlation entropy $K_2(M)$ versus the embedding dimension M for both the linear and non-linear signals. Crosses refer to the linear signal and circles to the non-linear process. The error bars on ν_M are the 95% confidence limits of the least-squares-fit slope of $\log C_M(r)$ versus $\log r$; the error bars on $K_2(M)$ are the standard deviation on the mean value of $[\log C_M(r) - \log C_{M+1}(r)]/\Delta t$ in the scaling range.

the scale range where the spectrum is power-law. Theiler also estimated a lower bound N_0 to the number of points required in order to observe the space-filling scaling regime; N_0 "may have to be extremely large for this regime to be achieved". The power spectral properties of the noises considered in the present paper are similar to those discussed in ref. [49]; note, however, that the signal generated by (2.9) has been defined through a non-linear stochastic differential equation (not by its spectrum) and that its Fourier phases are not independent. Tests for the presence of non-linearity (such as the BDM test [53]) should give a positive result. Nevertheless, the present results show that finding that a time series is *non-linear* is certainly not sufficient to infer the presence of low-dimensional deterministic dynamics.

Another class of random processes which provide a finite correlation dimension estimate is obtained by considering a white noise with randomly superposed jumps of random amplitude (a random saw-tooth). One realization of such a process is shown in fig. 3a. In this example, the

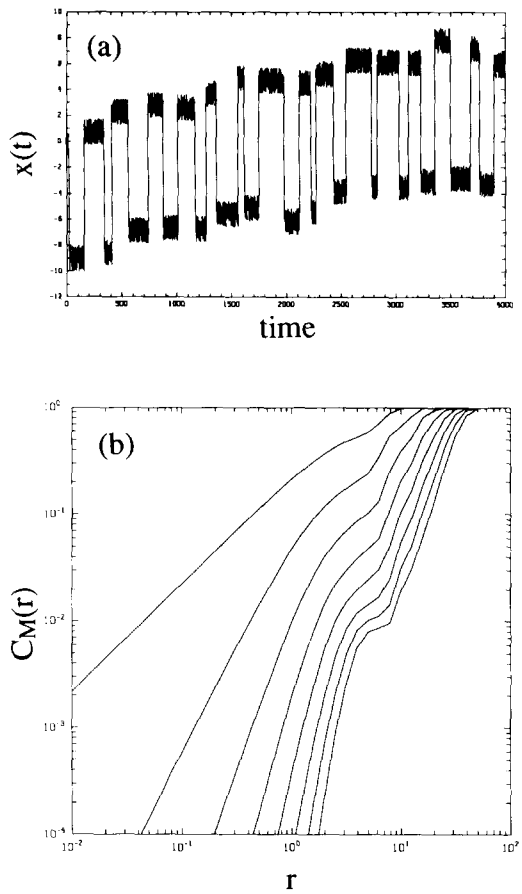

Fig. 3. (a) The "random saw-tooth" signal obtained by superposing random jumps of large amplitude onto a white noise background. (b) Correlation integrals $C_M(r)$ for the signal in fig. 3a; $\tau = 100\,\Delta t$ and $M = 1, \ldots, 8$.

"fast" dynamics is a white noise uniformly distributed between -1 and 1; we superposed onto it a random number of consecutively positive and negative jumps with amplitude $A_j = A_0 + \eta_j$, where $A_0 = 10$ and η_j is uniformly random distributed in $(-1, 1)$. The average time separation between jumps is about $100\,\Delta t$. The correlation integrals obtained from this time series are shown in fig. 3b; again, a value of the time delay corresponding to the first zero of the autocorrelation function has been chosen ($\tau = 100\,\Delta t$, here $\Delta t = 1$). A scaling regime in $C_M(r)$, with saturating correlation exponent, is clearly visible at large values of r for the higher embedding dimensions, leading to a correlation dimension $\nu \approx 2.7$. A similar structure was observed by Voges et al. [46] in the analysis of the X-ray variability of Hercules X-1 (their fig. 5); this behavior was ascribed to a two-amplitude-range process, where the low-amplitude fluctuations are due to high-dimensional dynamics and the large-amplitude fluctuations determined by a low-dimensional chaotic dynamics. However, such a behavior can be simulated by a purely stochastic process, as in the example above.

3. Some tests toward the goal of distinguishing between some chaos and some noise

The examples given in the previous section suggest that the distinction between low-dimensional dissipative chaos and (correlated) random noise should not be based solely on correlation dimension estimates. In addition to those considered here, other types of stochastic processes certainly exist which mimic the properties of low-dimensional chaos in finite data sets. Methods other than dimension calculations should be applied to measured time series in order to extract as much dynamical information as possible. In this regard, however, we recall that also predictability algorithms may have difficulty in distinguishing between chaos and correlated noise when a finite number of points is considered [21].

In a sense, simply examining the time series and its recurrence plots often indicates whether a meaningful correlation integral analysis can be performed (more precisely, such an examination often indicates the analysis should not be performed). For a system believed to contain a very-low-dimensional attractor (say, dimension less than three), one can directly inspect phase space trajectories and Poincaré sections; if these yield either "messy" distributions with no discernible structure or isolated, non-recurrent

patches of points, the correlation integral estimates should be interpreted with extreme caution. Analogously, time series which show rare bursts in otherwise unexplored regions of phase space, as well as an obvious non-stationarity and/or the absence of close returns in phase space are not promising candidates for the search of low-dimensional dissipative chaos.

Clearly, real time series are a mixture of deterministic components and random noise; it is nevertheless of some interest to attempt to disentangle the two components (when possible). In this section we discuss simple tests which may be applied to an experimental time series in order to interpret correlation dimension estimates and distinguish low-dimensional dynamics from stochastic processes. These tests are based on the idea of modifying some of the properties of a time series (i.e., on generating appropriate "surrogate" data, in a language similar to that used in refs. [26, 30]), in order to determine whether the convergence of the dimension and of the entropy (or some other measured quantity) does or not depend on the modified property.

It is important to stress the fact that each test *in se* is not an absolute proof; at best we are able to evaluate the probability that a series would produce the observed result by chance if it were chosen from an ensemble of signals with some given set of properties. These properties are chosen in an attempt to fool the algorithm tested and the usefulness of the test depends on the choice of good surrogate signals. The comparison between several of the above approaches increases the confidence in a distinction between chaos and noise. Finally, we recall that we tend to include in the term "randomness" the behavior of a dynamical system which cannot be represented in terms of a few active degrees of freedom, but which must instead be characterized by a large number of excited modes. The definitions of "few" and "large numbers" are vague and will depend on the level of technology and the theory available. This means that one will (mis)classify sufficiently "high" dimensional chaos as randomness.

3.1. Space–time-separation plots

The first test simply recasts the data in the correlation integral to make the bias due to dynamical correlations more obvious. We recall that Theiler [23] demonstrated that short-time correlations can produce "knees" in the correlation integral due to the one-dimensional nature of the trajectory. Analysis of fractal trajectories may result in similar knees with non-integer dimension.

The correlation integral represents the probability that a pair of randomly chosen points on the reconstruction will be less that a distance r apart. When making the standard calculations, one assumes the distance between pairs of points is due to the geometry of the reconstruction, *not* because the points are dynamically correlated and their separation in space reflects their being neighbors in time. These temporal correlations led Theiler to restrict the sums in eq. (2.2) to i, j pairs where $|i - j| > W$ for some constant W. The graphs presented below may be interpreted as providing a method for choosing W; in the case of non-stationary power-law noises they indicate that there is no value of W for which the correlation integral reflects global scaling due to recurrence.

For reconstructions from a single time series, each pair of points on the reconstruction is separated in phase space by some distance r and in time by some Δt. Our approach is to consider the time separation of points explicitly, first, through a scatter plot of the separation between two points in the space against their separation in time. This is illustrated for a three-dimensional reconstruction of the x series from the Lorenz equation [54] with $\sigma = 10$, $b = \frac{8}{3}$ and $r = 24.74$; in fig. 4 where the horizontal axis is separation in time and the vertical axis is the base 2 logarithm of the separation in space. For small Δt points

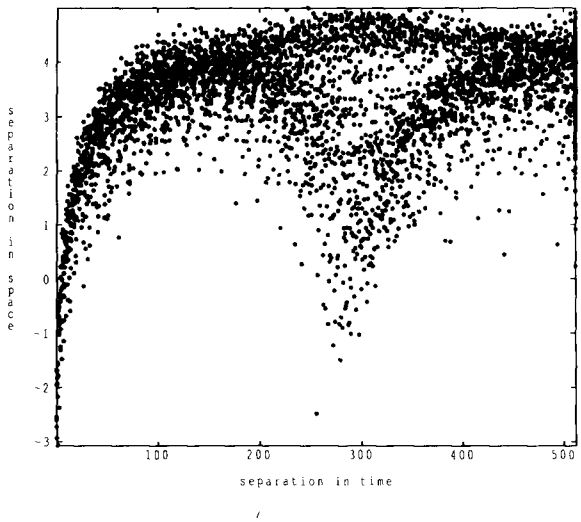

Fig. 4. Scatter plot of the spatial separation versus time separation between pairs of points on a trajectory on the Lorenz attractor. The horizontal axis is separation in time and the vertical axis is the (base 2 logarithm of) the separation in space.

are always near neighbors in space, as their time separation increases so, initially, does their separation in space.

For large data sets, scatter plots are difficult to interpret. An alternative is to plot contour maps of the fraction of points closer than a distance r at a given time separation Δt as a function of Δt, equivalently $P(|x(t+\Delta t)-x(t)|<r)$ for arbitrary t. For large N and Δt (in systems in which correlations decay with time), this distribution converges to the correlation integral for each Δt. The purpose of these contour maps is to observe the manner in which this convergence comes about.

Fig. 5 shows the space–time-separation contour map for the Lorenz case shown in fig. 4. The first zero of the autocorrelation function corresponds to 295 in the integer units of the graph. Fig. 5b shows the distribution over longer time scales. The length of time for which memory effects are significant is surprisingly long. The correlation integral is usually computed including these time separations with the implicit assumption that the visible oscillations average out.

Fig. 6 shows the corresponding results for a $1/f$ power-law noise. It is clear in this example that the only points with small spatial separation are dynamically near neighbors: The series is non-recurrent in phase space. The key point here is that there is no analogue of fig. 5b for the power-law noise signal: There exist no time scales on which the distribution is stable. As the correlation integral effectively projects this graph onto the vertical axis, biased estimates of the correlation integral will result when the contributions of this projection are disturbed by structure at small t. In the plots for the power-law noise this is always the case; whatever time threshold is chosen, the smallest length scales will always be dominated by the smallest time scales. For the Lorenz attractor, Theiler's approach removes the contribution of the region $|i-j|<W$; from fig. 5a it is clear that for, say, $W<32$ the distribution contains many near neighbors due to dynamical correlations. For a chaotic system, the decay of correlations with time results in the convergence of slices at constant Δt to the correlation integral at large Δt. The memory of initial conditions, reflected here in the persistence of long time structure of this plot is greater than might have been expected.

The connection with the correlation integral is straightforward: $C(r)$ is simply the sum over "large" Δt for a given r; the usefulness of this graph is that (a) it provides a quantitative estimate of what constitutes "large Δt" (namely those values where the contours have reached their asymptotic behavior), (b) it is sensitive to the specific reconstruction parameters used and the full non-linear structure in M dimensions as opposed to the (linear) autocorrelation function or the one-dimensional mutual information, and (c) computationally, it is a subset of the correlation integral. Note that these distributions may also be used to estimate the inside cutoff to scaling range in the spatial separation of points with minimal dynamic correlation.

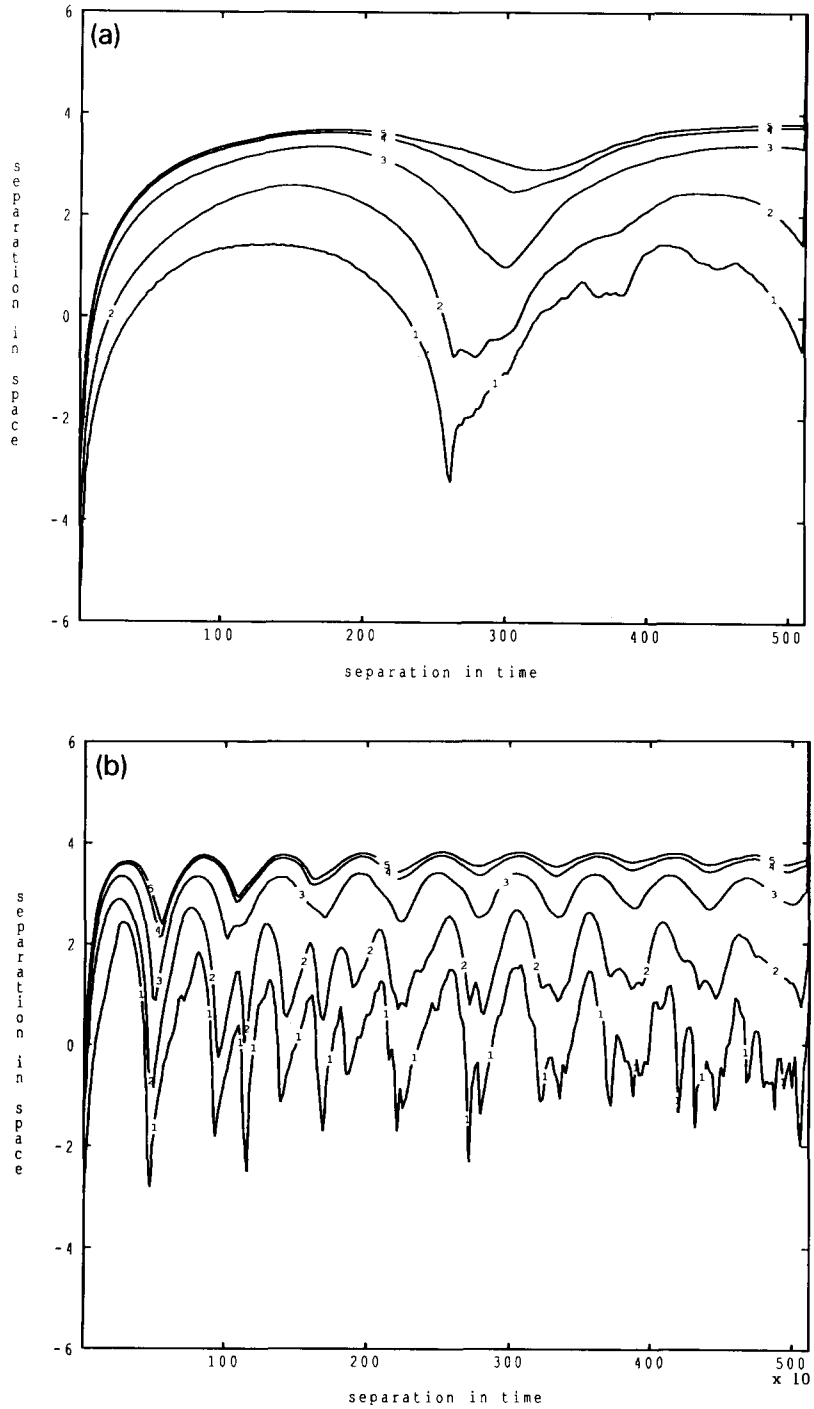

Fig. 5. Space–time-separation plots for the Lorenz attractor as in fig. 4. In this case the scatter diagram is replaced by a contour map at short time scales (a) and at longer time scales (b). The contours indicate the fraction of points closer than a distance r at a given time separation Δt. The different curves correspond to different fractions; curve 1 refer to a fraction of 1%, curve 2 to 10%, curve 3 to 50%, curve 4 to 90% and curve 5 to 99%.

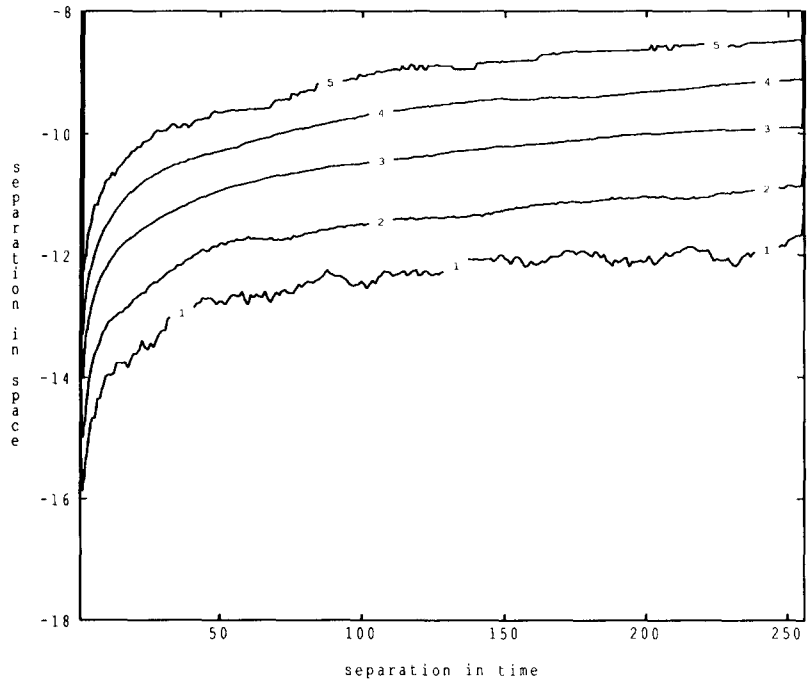

Fig. 6. Space–time-separation contour map for a $1/f$ power-law noise, as a function of Δt. Same details as in fig. 5.

For very long series with low sampling rates, the effects discussed here become small as one eventually finds near returns closer to a given point than its dynamical next neighbor. For reasonable sampling rates, however, the data set lengths required for this to occur can be extremely long.

The power-law noise is employed here as a clear example of a series which is non-recurrent in phase space. In this case, the non-stationarity of the signal should be obvious by inspection of the time series itself. The space–time-separation maps quantify the occurrence (or absence) of near returns in more subtle time series.

Finally, we note a secondary bias in the correlation integral when high sampling rates are used. Even when near neighbors of a given point are omitted from the calculation centered at that point, they can still bias the probability distribution centered on points far away in time. This appears as a change in the conditional probability $P(\Delta x_{ij} < r + \Delta r \,|\, \Delta x_{ij-1} < r)$ through the correlation of $x(t_{j-1})$ and $x(t_j)$ for arbitrarily large values of $i - j$.

3.2. Phase randomization

A very useful test is to consider the distribution of the Fourier phases of the signal under study. In fact, in the case of fractal noise processes the convergence of the correlation dimension is forced mainly by the shape of the power spectrum (consistent with the fact that both the power spectrum and the correlation integral are related to the second moment of the distribution), while for a low-dimensional dynamics phase correlations play an essential role. Thus, given an experimentally measured signal $x(t)$ thought to be chaotic, it is useful to consider the stochastic surrogate signals obtained by inverting a power spectrum exactly equal to that of the signal under study and random, independent and uniformly distributed Fourier phases. If the convergence is determined only by

the shape of the spectrum (equivalently, by the autocorrelation function), then the results are not affected by phase randomization; the invariance of the correlation dimension and entropy estimates under phase randomization strongly implies that these estimates are not indicative of low-dimensional dynamics. To our knowledge, this test was first applied in the study of the motion of freely drifting buoys in the Pacific Ocean [43].

As an example of this approach, in fig. 7a we show the time series obtained by randomizing the Fourier phases of the non-linear stochastic process shown in fig. 1b, and in fig. 7b we report the corresponding correlation integrals. The difference between the original and the phase-randomized time series is visually apparent, since the phase randomization has destroyed the delicate phase couplings associated with the intermittent and multifractal nature of the process (2.9). The average correlation dimension estimates, however, do not show any significant differences between the original (non-liner) and the phase-randomized (linearized) signal, as shown in fig. 7c, which reports ν_M versus M for the two time series. For both signals, the correlation dimension saturates at approximately the same value. By repeating this procedure over an ensemble of ten different surrogate signals, corresponding to different choices of the random phases, we have always obtained saturating correlation dimension estimates with mean value $\langle \nu \rangle = 2.65$ and standard deviation $\sigma_\nu = 0.17$ (at embedding dimension $M = 8$). In general, we have noted that the scatter in the saturation values of ν_M obtained for an analogous ensemble of ten surrogates of the linear signal (2.8) is smaller ($\langle \nu \rangle = 2.47$ and $\sigma_\nu = 0.08$ at $M = 8$); this difference, however, is in general not sufficient to infer the linear or non-linear nature of the original signal.

The above results can be understood by recalling that the correlation dimension is related to the second moment of the probability distribution associated with the time series (in a given embedding space), i.e., it is related to the autocorrelation or to the power spectrum. For a stochastic signal, the phase information determines the behavior of higher moments, i.e., it is related to the generalized fractal dimensions (as-

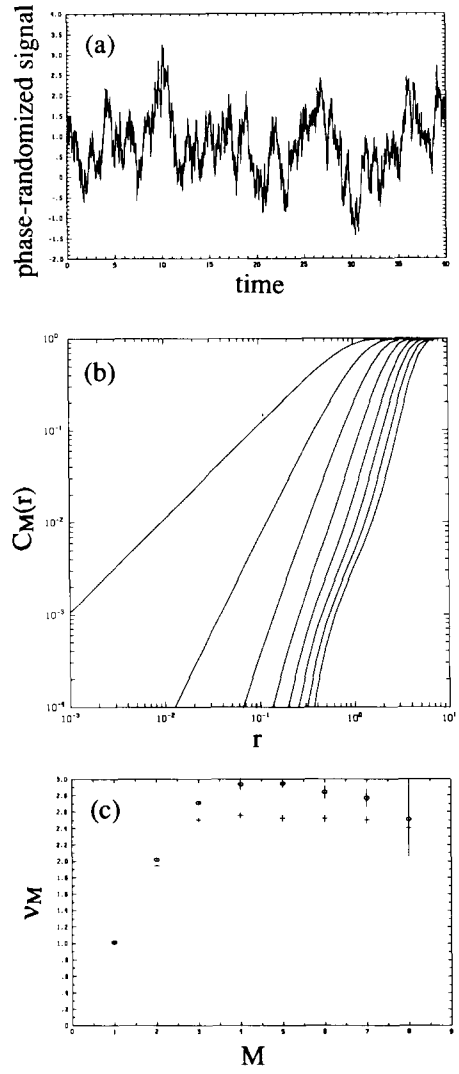

Fig. 7. (a) Signal obtained by randomizing the Fourier phases of the non-linear time series shown in fig. 1b. (b) Correlation integrals for the phase-randomized time series shown in fig. 7a; $\tau = 250\,\Delta t$ and $M = 1, \ldots, 8$. (c) Correlation exponent ν_M versus the embedding dimension M for the original (crosses) and phase randomized (circles) time series. Error bars are the 95% confidence limits on the least-squares fit.

sociated with the intermittency properties) and to higher-order spectral quantities such as the bispectrum. All these higher-order measures are obviously modified by phase randomization in the case of the non-linear signal. Along these lines, a useful test to detect the presence of non-linearity and phase correlations in a given stochastic signal is to verify how the spectrum of multifractal dimensions is changed under phase randomization [27]. Clearly, for the purpose of distinguishing between chaos and noise one should attempt to choose stochastic surrogates which resemble the original series as much as possible (even in the higher moments). For example, the sunspot series has a number of non-linear characteristics; in this case, rather than simply use phase randomization one might consider non-linear stochastic model simulations, as discussed in refs. [30, 55].

On the other hand, if the convergence is due to an underlying deterministic dynamics, phase randomization destroys the convergence of the dimension and of the entropy estimates. As an example, figs. 8a and 8b report a 4000-point time series of the x component from the Lorenz attractor, with the same parameters as above, before and after the phase randomization. The time step used is $\Delta t = 0.05$. The appearance of the two time series is completely different and the correlation dimension results differ as well, see figs. 8c and 8d. In fact, there is no clear scaling range in $C_M(r)$ for the phase-randomized signal, as shown in figs. 8e and 8f which report the local logarithmic slope of $C_M(r)$ for each case. For the phase-randomized signal, ν_M may be defined as an average slope over a specified range of length scales. Fig. 8g shows ν_M versus M for both signals; as one can see, the average correlation exponent for the phase-randomized signal does not saturate. By repeating the analysis over an ensemble of ten surrogate signals we have always obtained non-convergent correlation dimension estimates for the phase-randomized signals.

We caution, however, that a change in the correlation integrals under phase randomization does not necessarily imply the existence of an underlying strange attractor. For example, phase randomization of signals with strong periodic or quasi-periodic components in their spectrum will be more difficult to interpret. In principle, quasi-periodic signals with the geometry of tori can be detected by their integer dimension. In reality, however, the uncertainty in dimension estimates makes identifying integers impractical. Other tests better designed to identify signals such as these exist (see e.g. ref. [56]). The combined use of several methods is often a crucial step in the correct analysis of the source of difficulties with correlation integral techniques. Alternatively, the use of some noise-filtering algorithms [11, 15, 16] may help in elucidating the true nature of the system, although non-linear cleaning should be kept distinct from "bleaching" the data [26].

3.3. *Signal differentiation*

Another test considers the correlation integral analysis of the first (numerical) derivative of the signal. For a system governed by a low-dimension strange attractor, the value of the correlation dimension is the same for the original signal as well as for the first (or for a higher) derivative (note that the time delay may have to be modified). In the case of a stochastic signal, The first derivative (or difference) of the signal has a correlation dimension which, when well defined, is often much larger than that of the original signal, consistent with the change in the logarithmic spectral slope under signal differentiation. Fig. 9a reports the first difference signal $\Delta x(t) = x(t + \Delta t) - x(t)$ of the x component of the Lorenz attractor; fig. 9b reports the correlation integrals for $\Delta x(t)$ and fig. 9c shows the values of the correlation exponent versus the embedding dimension for the original time series and for the first difference signal $\Delta x(t)$. The same value of τ has been used for both time series ($\tau = 5\,\Delta t$,

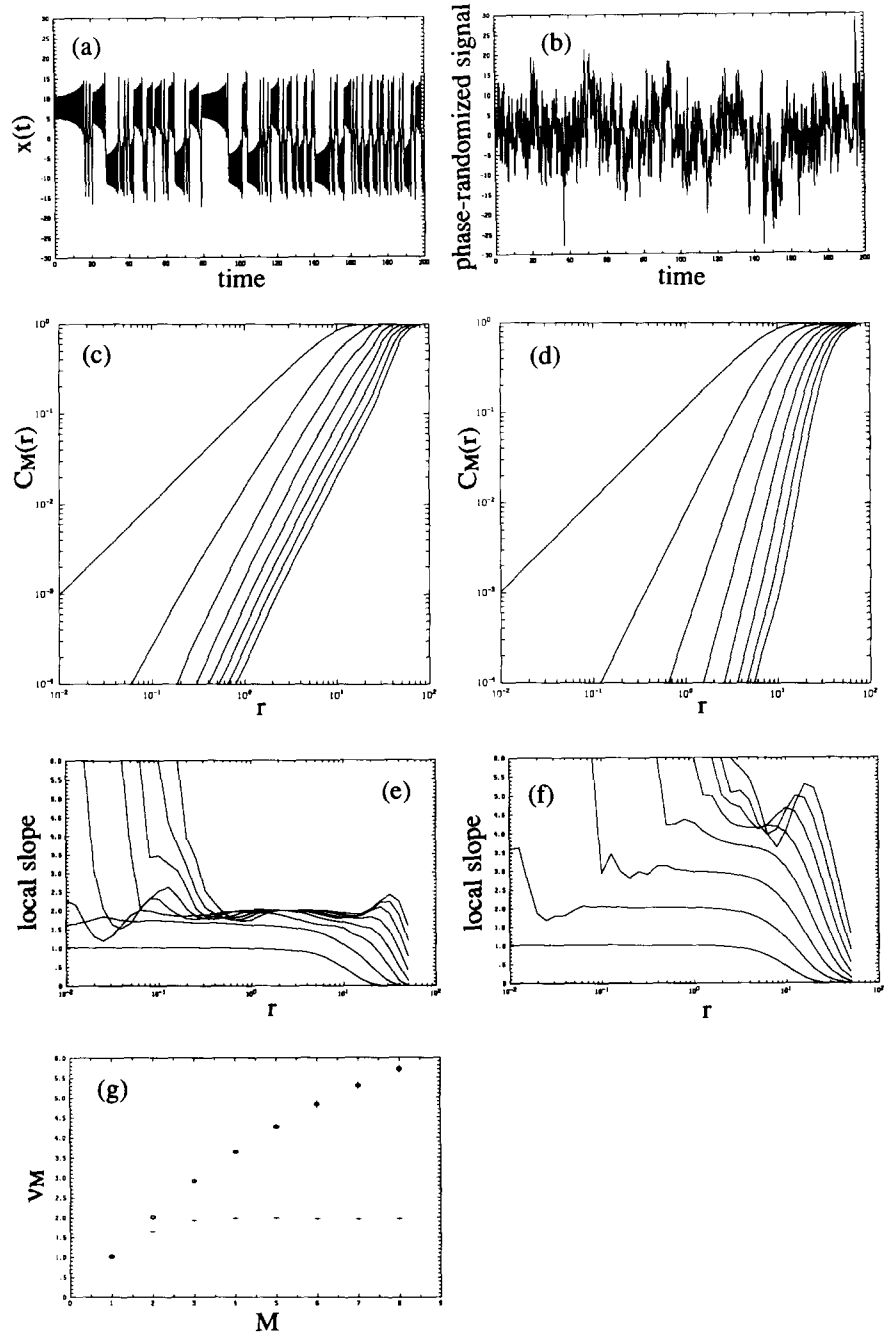

Fig. 8. (a) and (b) report respectively a time series obtained from the three-dimensional Lorenz model [28] and its phase-randomized counterpart; we use the standard values $\sigma = 10$, $b = 8/3$ and $r = 24.74$. A similar behavior is obtained for $r = 28$. The time step is $\Delta t = 0.05$. (c) and (d) report the corresponding correlation integrals with $\tau = 5\,\Delta t$ and $M = 1, \ldots, 8$; (c) and (f) report the local logarithmic slopes of the correlation integrals as obtained from a moving five-point linear regression of $\log C_M(r)$ versus $\log r$. (g) shows the (average) correlation exponent ν_M versus M for the original (crosses) and phase-randomized (circles) time series.

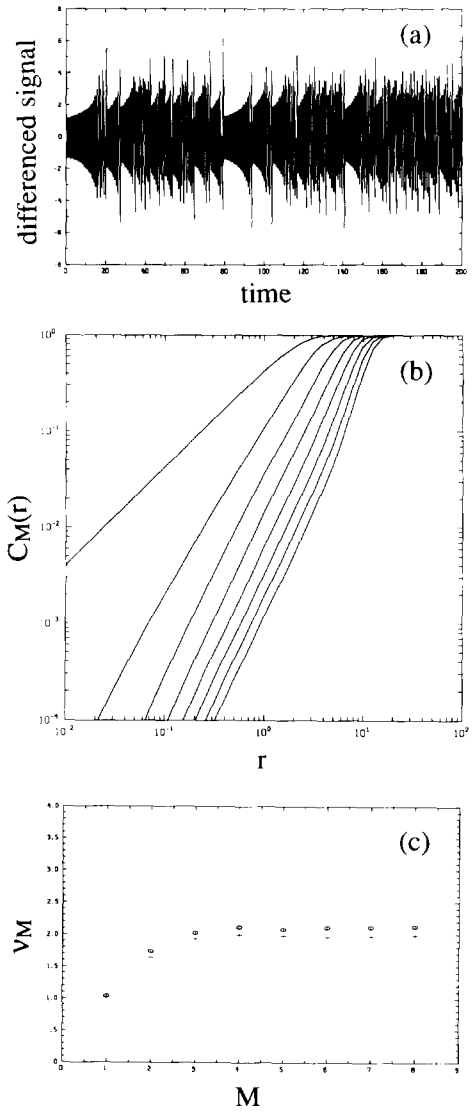

Fig. 9. (a) reports the first difference signal $\Delta x(t) = x(t + \Delta t) - x(t)$ obtained from the signal in fig. 8a, $\Delta t = 0.05$. (b) reports the correlation integrals for this signal, with $\tau = 5\,\Delta t$ and $M = 1, \ldots, 8$, and (c) reports the correlation exponents ν_M versus M for the original (crosses) and first difference (circles) signals.

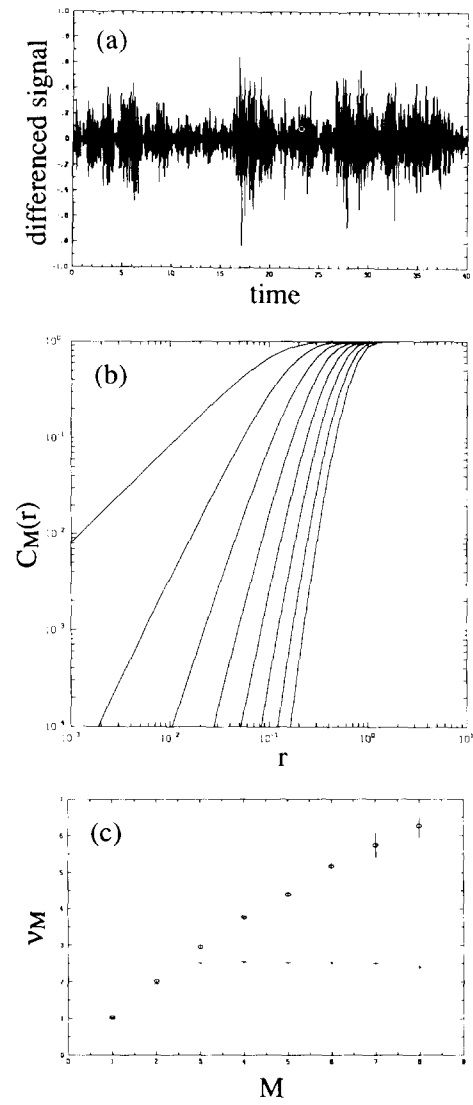

Fig. 10. (a) reports the first difference signal obtained from the non-linear stochastic process (2.9), $\alpha = \beta = 1$ and $\Delta t = 0.02$. (b) reports the corresponding correlation integrals for $\tau = 250\,\Delta t$ and $M = 1, \ldots, 8$. (c) shows the correlation exponent versus the embedding dimension for the original (crosses) and differenced (circles) signals. From panel (a) the intermittent nature of the process (2.9) is particularly evident.

where $\Delta t = 0.05$); as expected, results are very similar.

The first difference signal $\Delta y(t) = y(t + \Delta t) - y(t)$ obtained from the non-linear stochastic process (2.9) and the resulting analysis are shown in fig. 10; again, the same time delay $\tau = 250\,\Delta t$ has been used for both signals. As one can see, no saturation is observed in the correlation exponent of the difference signal. This is due to the fact that the increments $\Delta y(t)$ have essentially a white noise spectrum in this case, and have

consequently a much shorter correlation time. Thus, when a clear estimate of the derivative of a signal is available, the existence of a strong difference in the correlation dimension between the measured signal and its first derivative is a good indication that the dynamics has a significant stochastic component. Conversely, if the results of the correlation analysis do not change under signal differentiation, one has strong indication that the dynamics is not simply a fractal noise. Clearly, there may be severe difficulties in estimating the derivatives of measured signals.

Another possibility (similar in spirit to signal differentiation) is to consider a generic diffeomorphism $z = F\{x\}$ of the observed variable. For a sufficiently long series from a deterministic system, no difference should be observed between the correlation dimension of the signal $x(t)$ and that of $z(t)$, apart from the effects due to the amplification of measurement noise. In contrast, the dimension of a stochastic fractal signal should drastically change under this operation, since the characteristics of the process will be modified [34]. Changes in the correlation integrals may depend crucially upon $F\{x\}$; a careful examination of different classes of transformations must be pursued. We also note that transformation of the distribution (effectively, a change in the measurement function) has been applied by Theiler et al. [26].

3.4. Independent realizations

A useful test is based on considering several independent realizations of the dynamics, with different initial conditions. In the case of a low-dimensional dissipative dynamics, the correlation dimension of the set of points obtained by considering all realizations at once is equal to that of a single realization, provided that the different realizations start in the same basin of attraction. On the other hand, for a stochastic system the different realizations tend to fill the entire space, and one should observe an increase of the correlation dimension estimate with the number of realizations considered. In fact, the convergence of the dimension estimates for the noises considered here are due to the existence of long time correlations, the effect of which is diminished by considering *independent* realizations.

To illustrate this behavior, fig. 11a contrasts the correlation exponent versus the embedding dimension for a set obtained by combining five independent time series of the x component of the Lorenz attractor against the results for a single time series of the same total length. Fig. 11b reports the correlation exponent versus the embedding dimension for a set of points obtained by composing five independent realizations of the non-linear stochastic process (2.9), together with the correlation exponent obtained

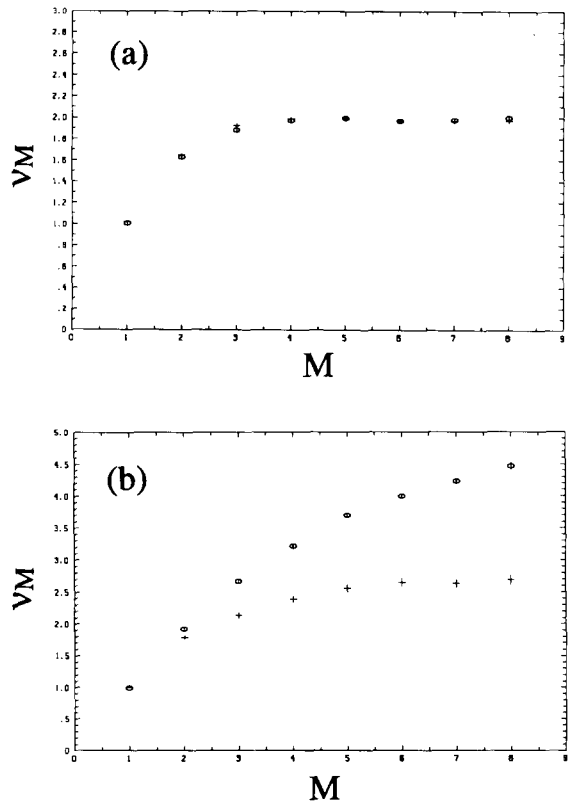

Fig. 11. Correlation exponent versus the embedding dimension for the Lorenz attractor (a) and for multiple realizations of the non-linear stochastic process (2.9) (b). Crosses are for a single realization, circles refer to the results obtained by superposing five independent realizations.

from the analysis of a single realization. The growth of the correlation dimension estimate with the number of realizations is clearly visible in this case. Another approach in this vein is to consider simultaneous measurement of several quantities. When the quantities measured reflect different aspects of the process, then the information content in two simultaneous signals of length T can be much greater than gaining "twice as many points" in either one of the signals by doubling the sampling rate (due in part to projection effects).

3.5. *Structure function*

A classic quantity in the study of measured time series is the structure function (SF), which is given by

$$S(n) = \sum_{i=1}^{N-n} [x(t + n\,\Delta t) - x(t)]^2 , \tag{3.1}$$

where $x(t)$ is a scalar signal. For a fractal signal, the structure function has a scaling behavior

$$S(n) \propto n^{2H} \tag{3.2}$$

at small values of n, where H is called the scaling exponent (see e.g. refs. [47, 57, 58]). A fractal signal whose SF is given by formula (3.2) has a power-law power spectrum $P(\omega) \approx \omega^{-\alpha}$, where $\alpha = 2H + 1$ [47]. By composing independent realizations $x_k(t)$ of a fractal signal on the different axes of an N-dimensional space, one obtains a fractal trajectory which is parametrically represented by the set of $x_k(t)$. The correlation dimension ν of the trajectory is related to the scaling exponent by the expression $\nu = 1/H$, if $\nu \leq M$ [47, 57, 58]. The different signals $x_k(t)$ may be independent realizations or time-delayed versions of the same signal.

The structure function of the stochastic processes (2.8) and (2.9) displays a scaling behavior

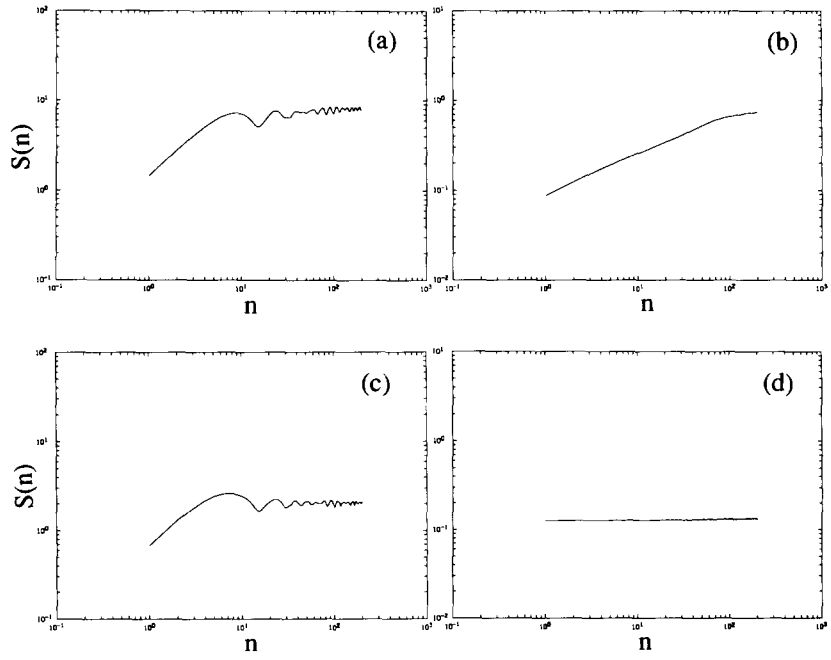

Fig. 12. (a) Structure function (SF) for the x component of the Lorenz attractor shown in fig. 8a. (b) SF for the non-linear stochastic process shown in fig. 1b. (c) SF for the first difference deterministic signal shown in fig. 9a. (d) SF for the first difference stochastic signal shown in fig. 10a.

of the kind (3.2) (at least on the time scales corresponding to the power-law regime in the spectrum). Alternatively, for motion on a strange attractor, which is differentiable in the direction of motion (and whose fractal structure is due to "close returns" in phase space), the SF has a scaling exponent $H = 1$ at small values of n. The SF tends to oscillate and then to become constant at increasing n, due to the limited region of the phase space visited by the system. As an example of the above statements, in fig. 12 we report the SF versus n for the x component of the Lorenz attractor (a) and for the non-linear noise (2.9) (b). The difference between the two structure functions is striking; the SF for the non-linear noise shows an extended scaling regime while the SF for the Lorenz attractor displays the typical behavior discussed above.

By combining the test of the signal differentiation and the SF calculation one obtains an even more clear difference between chaos and fractal noise. Fig. 12c shows the SF versus n for the first difference signal obtained from the x component of the Lorenz attractor and fig. 12d reports the SF for the first numerical derivative of the non-linear process (2.9). The SF of the differentiated signal from the Lorenz attractor is practically equal to that of the original time series, while the SF of the noise is now flat, indicating $H = 0$ and a non-convergent dimension estimate for the first differenced signal.

4. Discussion and conclusions

The (re)discovery of low-dimensional deterministic chaos and the development of data analysis methods which can be easily implemented have stimulated many works devoted to the study of experimental signals from the "chaotic" viewpoint. This work has often focused on deciding whether apparently unpredictable behavior should be ascribed to the presence of a low-dimensional strange attractor rather than "random" behavior. In many cases, however, the desire for finding a chaotic attractor has led to a naive application of the analysis methods; as a result, the number of claims on the presence of strange attractors in vastly different physical, chemical, biological and astronomical systems has grown (exponentially?). Difficulties in interpreting correlation integral results led for example Grassberger et al. [15] to state that ". . . most (if not all) of these claims have to be taken with very much caution". Analogously, in a more specific context, Lorenz [40], based on the analysis of a dynamical system with several *weakly coupled* degrees of freedom, has recently concluded that there is "no reason to believe that an extensive weather or climate system possesses a low-dimensional attractor".

The most convincing evidence for low-dimensional chaos most commonly arises when the spatial complexity of the system is limited. Examples include carefully controlled laboratory experiments, transitional regimes (for example from laminar to turbulent flows) and some natural systems where physical reasons clearly imply the presence of only a few active collective modes [39]. Extended systems (e.g. fluids) may require long (global) space correlations for a low-dimensional dynamics to exist. Systems with short space-correlations, as well as systems with weakly coupled phase space variables, need not be (globally) described by low-dimensional dynamics. For the latter systems, the standard correlation integral approach may (again in Lorenz's words) "attempt to measure the dimension of a subsystem" [40].

In this paper we have extended the results given in refs. [47, 48] and we have considered several different types of random noises which can result in convergent estimates of the dimension and of the entropy. In particular, we have considered two types of *stationary* stochastic processes, generated by linear and by non-linear stochastic processes. It has been shown that both noises provide a very similar output of the dimension and entropy (numerical!) estimates. These results are of some interest since they

remove the objection that only non-stationary noises are associated with convergent dimension and entropy estimates. In the case of stochastic signals, the convergence of dimension estimates are a result of the fractal nature of the trajectories. As it is crucial to distinguish which aspect of the signal the estimate is reflecting, we have examined this question directly through space–time-separation plots and structure functions.

Given the interest of distinguishing between low-dimensional chaos and random behavior in observed signals, we have considered a series of tests which can assist (or circumvent) the interpretation of the correlation integral. These tests employ appropriate surrogate data which must then be analysed by the same methods employed with the original time series to determine whether the estimates of the dimension, entropy or any other statistic depend on the characteristics of the time series which have been modified. In particular, we have considered the procedures based on randomizing the Fourier phases of the signal, numerically differentiating the original time series, and the analysis of several independent realizations of the same dynamics. We have also discussed how the structure function can be used for contrasting low-dimensional chaos and fractal noises. In general, we have shown that low-dimensional dynamics may be distinguished from fractal noises by using these tests. The case of randomly modulated periodic (or quasi-periodic) oscillations could be much more complicated, and a clear distinction between chaos and random modulations might best employ other techniques (see e.g. ref. [56]).

In conclusion, we stress that there is no simple test which automatically and unequivocally indicates the presence or the absence of chaotic dynamics; it is only through the comparison of several different methods that the dynamical processes underlying a given system may be assessed. As always, a minimal physical insight into the dynamics of the system under study is a great asset. In this regard, we think it would be extremely useful to produce a collection of signals (both deterministic and random) and provide a detailed description of the output of the various analysis techniques when applied to each of them. In this way, safer conclusions on the presence of chaos, low-dimensional dynamics and/or noise from the analysis of measured time series could be obtained.

Acknowledgements

The present work has benefitted by several discussion with Jean-Guy Caputo, Peter Grassberger, Mark Muldoon, James Theiler and Risheng Wang during the IUTAM Meeting on interpretation of time series from mechanical systems (Warwick University, UK, August 1991), as well as by fruitful visits of two of us (A.P. and L.S.) to Professor Klaus Fraedrich at the Free University of Berlin. L.S. would also like to acknowledge profitable discussions with Professor Mike Gaster which led to the space–time-separation graphs.

References

[1] H.D.I. Abarbanel, R. Brown and J.B. Kadtke, Phys. Rev. A 41 (1990) 1742.
[2] R. Badii and A. Politi, Phys. Rev. Lett. 52 (1984) 1661.
[3] D.S. Broomhead and G.P. King, Physica D 20 (1986) 217.
[4] D.S. Broomhead and R. Jones, Proc. R. Soc. London A 423 (1989) 103.
[5] M. Casdagli, Physica D 35 (1989) 335.
[6] M. Casdagli, S. Eubank, J.D. Farmer and J. Gibson, Physica D 51 (1991) 52.
[7] J.P. Crutchfield and B.S. McNamara, Compl. Syst. 1 (1987) 417.
[8] J.-P. Eckmann and D. Ruelle, Rev. Mod. Phys. 57 (1985) 617.
[9] J.-P. Eckmann, S. Oliffson Kamphorst, D. Ruelle and S. Ciliberto, Phys. Rev. A 34 (1986) 4971.
[10] J.D. Farmer and J.J. Sidorovich, Phys. Rev. Lett. 59 (1987) 845.
[11] J.D. Farmer and J.J. Sidorovich, Physica D 47 (1991) 373.
[12] P. Grassberger and I. Procaccia, Physica D 9 (1983) 189.

[13] P. Grassberger and I. Procaccia, Phys. Rev. A 28 (1983) 2591.
[14] P. Grassberger, Phys. Lett. A 148 (1990) 63.
[15] P. Grassberger, T. Schreiber and C. Schafrath, preprint (1991).
[16] E.J. Kostelich and J.A. Yorke, Phys. Rev. A 38 (1988) 1649.
[17] W. Liebert and H.G. Schuster, Phys. Lett. A 142 (1989) 107.
[18] M. Sano and Y. Sawada, Phys. Rev. Lett. 55 (1985) 1082.
[19] T. Sauer, J.A. Yorke and M. Casdagli, J. Stat. Phys. 65 (1991) 579.
[20] L.A. Smith, Phys. Lett. A 133 (1988) 283.
[21] G. Sugihara and R.M. May, Nature 344 (1990) 734.
[22] F. Takens, Detecting strange attractors in turbulence, in: Lecture Notes in Mathematics, Vol. 898, eds. D.A. Rand and L.S. Young (Springer, Berlin, 1981) p. 366.
[23] J. Theiler, Phys. Rev. A 34 (1986) 2427.
[24] J. Theiler, Phys. Rev. A 36 (1987) 4456.
[25] J. Theiler, J. Opt. Soc. Am. A 7 (1990) 1055.
[26] J. Theiler, B. Galdrikian, A. Longtin, S. Eubank and J.D. Farmer, Los Alamos Preprint LA-UR-91-2615 (1991).
[27] R. Vio, S. Cristiani, O. Lessi and A. Provenzale, Time series analysis in astronomy: an application to quasar variability studies, Astrophys. J., in press (1992).
[28] A. Wolf, J.B. Swift, H.L. Swinney and J.A. Vastano, Physica D 16 (1985) 285.
[29] N.H. Packard, J.P. Crutchfield, J.D. Farmer and R.S. Shaw, Phys. Rev. Lett. 45 (1980) 712.
[30] L.A. Smith, Physica D, submitted.
[31] P. Atten, J.G. Caputo, B. Malraison and Y. Gagne, J. Mech. Theor. Appl., Special Issue (1984) 133.
[32] A. Brandstater, J. Swift, H.L. Swinney, A. Wolf, J.D. Farmer, E. Jen and P.J. Crutchfield, Phys. Rev. Lett. 51 (1983) 1442.
[33] S. Cilberto and J.P. Gollub, J. Fluid Mech. 158 (1985) 381.
[34] J.K. Cannizzo, D.A. Goodings and J.A. Mattei, Astrophys. J. 357 (1990) 235.
[35] K. Fraedrich, J. Atmos. Sci. 43 (1986) 419.
[36] P. Grassberger, Nature 323 (1986) 609; 326 (1986) 524.
[37] A.K. Harding, T. Shinbrot and J.M. Cordes, Astrophys. J. 353 (1990) 588.
[38] C.L. Keppenne and C. Nicolis, J. Atmos. Sci. 46 (1989) 2356.
[39] Z. Kollath, Mon. Not. R. Astron. Soc. 247 (1990) 377.
[40] E.N. Lorenz, Nature 353 (1991) 241.
[41] C. Nicolis and G. Nicolis, Nature 311 (1984) 529.
[42] J.P. Norris and T.A. Matilsky, Astrophys. J. 346 (1989) 912.
[43] A.R. Osborne, A.D. Kirwan, A. Provenzale and L. Bergamasco, Physica D 23 (1986) 75.
[44] L.-H. Shan, P. Hansen, C.K. Goertz and R.A. Smith, Geophys. Res. Lett. 18 (1991) 147.
[45] A.A. Tsonis and J.B. Elsner, Nature 333 (1988) 545.
[46] W. Voges, H. Atmanspacher and H. Scheingraber, Astrophys. J. 320 (1987) 794.
[47] A.R. Osborne and A. Provenzale, Physica D 35 (1989) 357.
[48] A. Provenzale, A.R. Osborne and R. Soj, Physica D 47 (1991) 361.
[49] J. Theiler, Phys. Lett. A 155 (1991) 480.
[50] A.M. Fraser and H.L. Swinney, Phys. Rev. A 33 (1986) 1134.
[51] L.A. Smith, J.-D. Fournier and E.A. Spiegel, Phys. Lett. A 114 (1986) 465.
[52] T. Ozaki, in: Handbook of statistics, eds. E.J. Hannah and P.R. Krishnaiah (Elsevier, Amsterdam, 1985).
[53] W. Brock, W. Dechert and J. Scheinkman, A test for independence based on the correlation dimension, University of Wisconsin-Madison, SSRI paper 8702.
[54] E.N. Lorenz, J. Atmos. Sci. 20 (1963) 130.
[55] N. Weiss, Phil. Trans. R. Soc. London A 330 (1989).
[56] G.L. Bretthorst Bayesian spectral analysis and parameter estimation, Lecture Notes in Statistics (Springer, Berlin, 1988).
[57] B.B. Mandelbrot, The fractal geometry of nature (Freeman, San Francisco, 1982).
[58] A. Provenzale, A.R. Osborne, A.D. Kirwan and L. Bergamasco, The study of fluid parcel trajectories in large-scale ocean flows, in: Nonlinear topics in ocean physics, ed. A.R. Osborne (Elsevier, Amsterdam, 1991).